

Direct search for the Higgs boson to charm coupling at ATLAS

A. J. COSTA ON BEHALF OF THE ATLAS COLLABORATION

University of Birmingham, Birmingham, UK

Summary. — A direct search for the Standard Model Higgs boson decays to a pair of charm quarks is presented. This analysis uses the full LHC Run 2 dataset collected with the ATLAS detector, corresponding to an integrated luminosity of 139 inverse femtobarns of proton-proton collisions at a centre-of-mass energy of 13 TeV. An extrapolation of this search to the HL-LHC conditions (centre-of-mass energy of 14 TeV, integrated luminosity of 3000 inverse femtobarns) is also presented. The production of the Higgs boson in association with a W or Z boson decaying leptonically is measured. Flavour jet tagging algorithms are used to identify the signature of the Higgs boson decay to charm quarks, while reducing contamination from Higgs boson decays to bottom quarks. This search improves the constraint on the cross section times branching fraction for a Standard Model Higgs boson previously presented by ATLAS, using an integrated luminosity of 36 inverse femtobarns of proton-proton collisions at the same centre-of-mass energy. A constraint on the charm Yukawa coupling modifier from Higgs boson to charm quark decays is also set. The HL-LHC extrapolation of this search further improved the expected constraints.

PACS 14.80.Bn – Standard-model Higgs bosons.

1. – Introduction

The discovery of a particle with a mass of 125 GeV compatible with the Standard Model Higgs boson, H , by the ATLAS [1] and CMS [2] collaborations at the LHC [3] marked the beginning of studies of its properties. The couplings of the Higgs field to quarks and leptons - the Yukawa couplings - are a potential source of the fermion masses and have been probed since. The coupling of the Higgs boson to the 3rd generation of fermions was observed by both the ATLAS [4-6] and CMS collaborations [7-9], and

evidence for the interaction of the Higgs boson to muons was found by CMS [10], with ATLAS [11] finding a 2σ excess over the background-only prediction.

The interactions between the Higgs boson and the fermions do not constitute a mechanism resulting in the observed disparities between the fermion masses, nor it is guaranteed all couplings follow the Standard Model (SM) prediction. It is therefore of the utmost importance to measure all Higgs boson couplings to fermions.

The SM predicts a branching fraction of 2.9% [12] for the Higgs boson to charm decays, $H \rightarrow c\bar{c}$, representing one of largest contributions to the Higgs boson width (by SM expectations) yet to be established experimentally.

In the SM the Higgs-charm Yukawa coupling is expected to be five times smaller than the Higgs coupling to bottom quarks, $Hb\bar{b}$. While the Higgs-charm coupling is rather small, it is susceptible to significant modifications in some new physics scenarios [13-19].

Different approaches can be taken to measure the Higgs coupling to charm quarks [20-25], with this work focusing on the direct search for the decay. Previous and current analyses are built around the use of c -jet tagging algorithms, and the production of the Higgs boson in association with a vector (W/Z) boson is targeted, with the W/Z boson decaying leptonically. This allows for a convenient trigger strategy based on charged leptons or missing transverse energy present in the events, suppressing multi-jet backgrounds and enhancing the signal over background ratio with respect to the inclusive Higgs boson production.

The ATLAS collaboration performed an analysis using 36 fb^{-1} of proton-proton collision data at $\sqrt{s} = 13 \text{ TeV}$ and targeting $Z(\rightarrow \ell\ell)H(\rightarrow c\bar{c})$ production [22], obtaining an observed (expected) upper limit on the cross-section times branching fraction of $110 (150^{+80}_{-40})$ times the Standard Model expectation. The ATLAS search [23] presented in this work covers the $Z(\rightarrow \nu\nu)H(\rightarrow c\bar{c})$, $W(\rightarrow \ell\nu)H(\rightarrow c\bar{c})$ and $Z(\rightarrow \ell\ell)H(\rightarrow c\bar{c})$ production modes, making use of 139 fb^{-1} of proton-proton collision data at $\sqrt{s} = 13 \text{ TeV}$ collected between 2015 and 2018 with the ATLAS detector [26]. Equivalent searches have been performed by the CMS collaboration, with 35.9 fb^{-1} [24] and 138 fb^{-1} [25] of proton-proton collision data at $\sqrt{s} = 13 \text{ TeV}$.

2. – Analysis

In the ATLAS $VH(H \rightarrow c\bar{c})$ search [23] presented in this work events are categorised according to the number of charged leptons resulting from the vector boson's decay, defining the 0-, 1- and 2-lepton channels. The phase-space is further split in terms of the transverse momentum of the vector boson ($V = Z, W$) produced in association with the Higgs boson, p_T^V , resulting in two possible regimes: $75 \text{ GeV} < p_T^V < 150 \text{ GeV}$ and $p_T^V > 150 \text{ GeV}$.

Jets are tagged using two jet flavour tagging algorithms, DL1 and MV2c10 [27], with the former being a c -tagger, and the latter a b -tagger used for b -jet vetoes with a 70% b -jet efficiency working point also used in the ATLAS $VH(H \rightarrow b\bar{b})$ analysis [28]. From

these two algorithms a dedicated working point, optimised for the analysis, was built, with an associated efficiency of 27%, 8% and 1.6% for c , b and *light*-jets respectively. The efficiency in data is measured relative to simulation as a “scale factor”, using control samples of $t\bar{t}$ and Z + jets events and methods identical to those applied to b -tagging algorithms [27, 29, 30]. The scale factors have a typical precision of 5 - 10% and are generally consistent with unity. For a jet to be considered “ c -tagged” it must pass both conditions, *i.e.*, have a c -tag with a b -veto.

The two highest- p_T jets in each event are used to reconstruct the Higgs boson invariant mass, $m_{c\bar{c}}$, from which the signal is extracted. Additional jets to the two forming the Higgs boson candidate have to satisfy a b -tag veto. The $VH(H \rightarrow c\bar{c})$ signal regions are therefore orthogonal to the ones in $VH(H \rightarrow b\bar{b})$, as these use two b -tagged jets, allowing for a combination of the two analyses.

Events with two or more jets are considered, and are classified depending on the number of c -tagged jets, with 1 and 2 c -tags categories being considered. The complete event categorisation of the signal sensitive regions is summarised in Table I. Requirements on the angular distance between the two Higgs boson candidate jets, ΔR_{jj} , is applied on these regions in order to optimise the analysis sensitivity to the $VH(H \rightarrow c\bar{c})$ signal.

TABLE I. – *Summary of event categorisation of signal sensitive regions.*

| Channel | Tag Categories | Number of Jets | p_T^V |
|----------|-------------------|----------------|--|
| 0 lepton | 1 and 2 c -tags | 2 and 3 jets | $p_T^V > 150$ GeV |
| 1 lepton | | | |
| 2 lepton | | 2 and 3+ jets | $75 \text{ GeV} < p_T^V < 150 \text{ GeV}$ |
| | | | $p_T^V > 150 \text{ GeV}$ |

Control regions used to constrain the modelling of the V +jets background normalisations and shapes select events failing the ΔR_{jj} requirements in the signal regions. Top control regions are defined to constrain the modelling of $t\bar{t}$ and single-top processes, using events with one c -tag in the two highest- p_T jets and one third additional jet b -tagged in the 0-/1-lepton channels, and events with an $e\mu$ pair with opposite charges in the 2-lepton channel. Events with no Higgs candidate jets c -tagged and no additional jets b -tagged are used to constrain the normalisation of the V +jets light flavour component.

A binned maximum-profile-likelihood fit to the $m_{c\bar{c}}$ distribution is performed in the analysis categories (16 signal regions and 28 control regions), measuring simultaneously the signal strengths for the $VH(H \rightarrow c\bar{c})$, $VW(W \rightarrow cq)$ and $VZ(Z \rightarrow c\bar{c})$ processes. Each signal strength is defined as the ratio between the measured signal yield and the SM prediction, $\mu = \frac{(\sigma \times BR)_{\text{Observed}}}{(\sigma \times BR)_{\text{SM}}}$. A validation of the 1 c -tag (2 c -tag) categories is provided through the VW (VZ) signal measurements.

Systematic uncertainties are included in the fit as nuisance parameters, comprising theoretical uncertainties, detector systematics, signal and background modelling uncertainties and statistical uncertainties in the simulation samples for the signals and backgrounds. These can modify the shape and/or normalisation of the distributions. The normalisation of the main backgrounds (Z +jets, W +jets and top processes) is allowed to float freely in the fit and is obtained from the data. A separate floating normalisation for the top processes is used in the 2-lepton channel with respect to the other channels.

The fitted $VH(H \rightarrow c\bar{c})$ signal strength is $\mu_{VH(H \rightarrow c\bar{c})} = -9 \pm 15$. The diboson signal strengths are measured to be $\mu_{VZ(Z \rightarrow c\bar{c})} = 1.16^{+0.50}_{-0.46}$ and $\mu_{VW(W \rightarrow cq)} = 0.83^{+0.25}_{-0.23}$ with respective observed (expected) significances of 2.6 (2.2) and 3.8 (4.6) standard deviations over the background-only prediction.

An upper limit on $\mu_{VH(H \rightarrow c\bar{c})}$ of 26 (31^{+12}_{-8}) is observed (expected) at 95% CL using a modified frequentist CLs method [31]. The limits for the combined and individual lepton channels, with the latter coming from a fit with the $VH(H \rightarrow c\bar{c})$ signal strength decorrelated between lepton channels, can be found in Fig. 1.

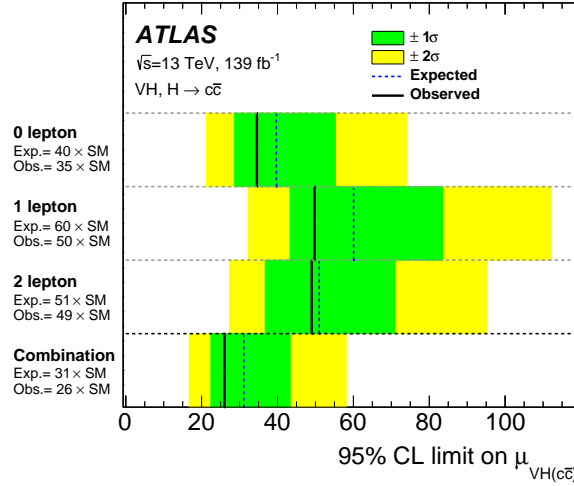


Fig. 1. – Observed and expected 95% CL upper limits on $\mu_{VH(H \rightarrow c\bar{c})}$ [23].

The dominant uncertainties on $\mu_{VH(H \rightarrow c\bar{c})}$ come from the modelling of the main backgrounds (V +jets and top processes), the statistical uncertainty from the limited size of the simulated samples and the jet flavour tagging uncertainties. The contribution of the systematic uncertainties to the $VH(H \rightarrow c\bar{c})$ signal strength is of similar magnitude to the statistical counterpart. The sensitivity to the diboson signals is limited by the systematic uncertainties, which follow a similar hierarchy of contributions to the $VH(H \rightarrow c\bar{c})$ case.

The $VH(H \rightarrow c\bar{c})$ signal strength is re-parameterised in terms of the κ_c coupling modifier [32, 33] for the Higgs boson-charm quark interaction, with the remaining coupling

modifiers set to unity (SM expectation), assuming no beyond-the-standard-model contributions to the Higgs boson width and considering only modifications to the Higgs boson decay. The signal strength is therefore defined as $\mu_{VH(H \rightarrow c\bar{c})}(\kappa_c) = \frac{\kappa_c^2}{1 + BR_{H \rightarrow c\bar{c}}^{SM}(\kappa_c^2 - 1)}$. An observed (expected) upper limit of $|\kappa_c| \leq 8.5$ (12.4) is set at 95% CL.

A combination of this $VH(H \rightarrow c\bar{c})$ analysis with the $VH(H \rightarrow b\bar{b})$ measurement [28] is realised. This allows for the measurement of the ratio of coupling modifiers κ_c/κ_b without assumptions on the Higgs boson width, as for the correlation of the common experimental systematic uncertainties between the two analyses. The jet flavour tagging and background modelling uncertainties are kept uncorrelated due to different implementations or parametrisations in the two cases.

A profile likelihood scan on κ_c/κ_b allows for an observed (expected) constraint of $|\kappa_c/\kappa_b| \leq 4.5$ (5.1) at 95% CL to be set, as shown in Fig. 2. Given the ratio of the bottom- and charm-quark masses being equal to $m_b(m_H)/m_c(m_H) = 4.578 \pm 0.008$ [34], this result constrains the Higgs boson coupling to charm quarks to be weaker than its coupling to bottom quarks at 95% CL.

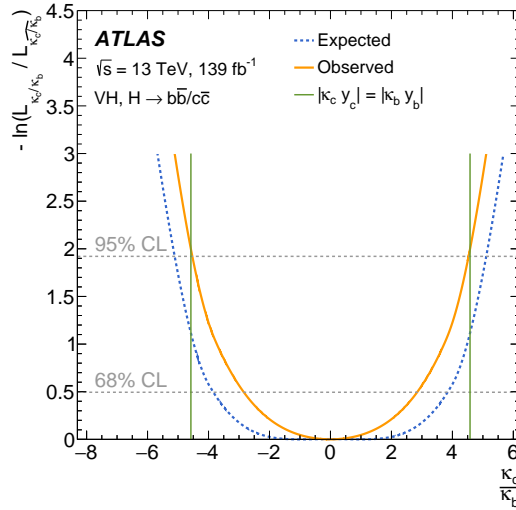


Fig. 2. – Observed and expected constraints from a profile likelihood scan on $|\kappa_c/\kappa_b|$ at 95% CL, where κ_b is a free parameter. A scenario with an equal coupling of the Higgs boson to charm and bottom quarks is represented by green lines, corresponding to the ratio $|\kappa_c/\kappa_b| = m_b/m_c$ [23].

An extrapolation of the $VH(H \rightarrow c\bar{c})$ and $VH(H \rightarrow b\bar{b})$ analyses to the High-Luminosity LHC (HL-LHC) scenario is performed [35], based on an expected centre-of-mass energy $\sqrt{s} = 14$ TeV and a total integrated luminosity of 3000 fb^{-1} .

The normalisations of the signal and background expected yields are scaled for the increase in integrated luminosity from 139 fb^{-1} to 3000 fb^{-1} . To account for the increase in centre-of-mass energy, the $qq \rightarrow WH$, $qq \rightarrow ZH$ and $gg \rightarrow ZH$ signal yields are scaled

by a factor 1.10, 1.11 and 1.18, respectively. The $t\bar{t}$ and $gg \rightarrow ZZ$ background yields increase by a factor 1.16, while the $qq \rightarrow VV$, V +jets and single top processes yields are scaled by a factor 1.10 [33].

The theory, background modelling and jet flavour tagging (with the exception of the light-jets component in the $VH(H \rightarrow c\bar{c})$ analysis) uncertainties are scaled by a factor 0.5. Uncertainties associated with the limited size of simulated samples are not considered.

The extrapolation of the $VH(H \rightarrow c\bar{c})$ leads to an expected upper limit on $\mu_{VH(H \rightarrow c\bar{c})}$ of $6.4 \times \text{SM}$ at 95% CL. An expected constraint of $|\kappa_c| \leq 3$ at 95% is also obtained. The leading uncertainties on these expected constraints come from the Z +jets modelling and the flavour tagging uncertainties. Extrapolating the combination of the $VH(H \rightarrow c\bar{c})$ and $VH(H \rightarrow b\bar{b})$ analyses allows for an expected constraint of $|\kappa_c/\kappa_b| \leq 2.7$ at 95% CL to be set.

3. – Conclusions

This work reports the $VH(H \rightarrow c\bar{c})$ analysis at $\sqrt{s} = 13$ TeV using 139 fb^{-1} of proton-proton collision data recorded by the ATLAS detector at the LHC. Through the use of multivariate jet flavour tagging algorithms, an optimised event selection and categorisation, and a larger dataset, this search improves by a factor five on the previous limit obtained by the ATLAS experiment, setting an observed (expected) upper limit on $\mu_{VH(H \rightarrow c\bar{c})}$ of $26 (31_{-8}^{+12})$ at 95% CL.

A combination of the $VH(H \rightarrow c\bar{c})$ and $VH(H \rightarrow b\bar{b})$ analyses results in an observed (expected) constraint on the coupling modifiers $|\kappa_c/\kappa_b| \leq 4.5 (5.1)$ at 95% CL, without assumptions on the Higgs boson width. This constrains the Higgs boson coupling to the charm quark to be weaker than the coupling of the Higgs boson to the bottom quark at 95% CL, as this ratio is smaller than the ratio of the bottom- and charm-quark masses, m_b/m_c .

The extrapolation of the individual $VH(H \rightarrow c\bar{c})$ analysis and of its combination with the $VH(H \rightarrow b\bar{b})$ search demonstrates room for future improvements, as the Run 2 analyses extrapolated to HL-LHC conditions are not sensitive enough to test the SM predictions. Changes on the analysis design, better flavour tagging performance and further reductions of the background modelling uncertainties were not considered in extrapolation, and are possibilities for the future which would result in improved sensitivity at the HL-LHC.

REFERENCES

- [1] ATLAS COLLABORATION, *Phys. Lett. B*, **716** (2012) 1.
- [2] CMS COLLABORATION, *Phys. Lett. B*, **716** (2012) 30.
- [3] L. EVANS AND P. BRYANT, *JINST*, **3** (2008) S08001.
- [4] ATLAS COLLABORATION, *Phys. Rev. D*, **99** (2019) 072001.

- [5] ATLAS COLLABORATION, *Phys. Lett. B*, **786** (2018) 59.
- [6] ATLAS COLLABORATION, *Phys. Lett. B*, **784** (2018) 173.
- [7] CMS COLLABORATION, *Phys. Lett. B*, **779** (2018) 283. *Phys. Lett. B* 779 (2018) 283
- [8] CMS COLLABORATION, *Phys. Rev. Lett.*, **121** (2018) 121801.
- [9] CMS COLLABORATION, *Phys. Rev. Lett.*, **120** (2018) 231801.
- [10] CMS COLLABORATION, *JHEP*, **01** (2021) 148.
- [11] ATLAS COLLABORATION, *Phys. Lett. B*, **812** (2021) 135980.
- [12] A. DJOUADI, J. KALINOWSKI AND M. SPIRA, *Comput. Phys. Commun.*, **108** (1998) 56.
- [13] C. DELAUNAY, T. GOLLING, G. PEREZ AND Y. SOREQ, *Phys. Rev. D*, **89** (2014) 033014.
- [14] G. PEREZ, Y. SOREQ, E. STAMOU AND K. TOBIOKA, *Phys. Rev. D*, **92** (2015) 033016.
- [15] F. BOTELLA, G. BRANCO, M. REBELO AND J. SILVA-MARCOS, *Phys. Rev. D*, **94** (2016) 115031.
- [16] S. BAR-SHALOM AND A. SONI, *Phys. Rev. D*, **98** (2018) 055001.
- [17] D. GHOSH, R. S. GUPTA AND G. PEREZ, *Phys. Lett. B*, **755** (2016) 504.
- [18] D. EGANA-UGRINOVIC, S. HOMILLER AND P. R. MEADE, *Phys. Rev. Lett.*, **123** (2019) 031802.
- [19] D. EGANA-UGRINOVIC, S. HOMILLER AND P. R. MEADE, *Phys. Rev. D*, **100** (2019) 115041.
- [20] GEOFFREY BODWIN, FRANK PETRIELLO, STOYAN STOYNEV, AND MAYDA VELASCO, *Phys. Rev. D*, **88** (2013) 053003.
- [21] FADY BISHARA, ULRICH HAISCH, PIER FRANCESCO MONNI, AND EMANUELE RE, *Phys. Rev. Lett.*, **118** (2017) 121801.
- [22] ATLAS COLLABORATION, *Phys. Rev. A*, **120** (2018) 21, 211802.
- [23] ATLAS COLLABORATION, CERN-EP-2021-251 (2021).
- [24] CMS COLLABORATION, *JHEP*, **03** (2020) 131.
- [25] CMS COLLABORATION, CMS-PAS-HIG-21-008 (2022).
- [26] ATLAS COLLABORATION, *JINST*, **3** (2008) S08001.
- [27] ATLAS COLLABORATION, *Eur. Phys. J. C*, **79** (2019) 970.
- [28] ATLAS COLLABORATION, *Eur. Phys. J. C*, **81** (2021) 178.
- [29] ATLAS COLLABORATION, ATLAS-CONF-2018-001 (2018).
- [30] ATLAS COLLABORATION, ATLAS-CONF-2018-006 (2018).
- [31] A. L. READ, *J. Phys. G*, **28** (2002) 2693.
- [32] LHC HIGGS CROSS SECTION WORKING GROUP, S. HEINEMEYER, C. MARIOTTI, G. PASSARINO AND R. TANAKA (Eds.), CERN-2013-004 (2013).
- [33] LHC HIGGS CROSS SECTION WORKING GROUP, D. DE FLORIAN, C. GROJEAN, F. MALTONI, C. MARIOTTI, A. NIKITENKO, M. PIERI, P. SAVARD, M. SCHUMACHER, R. TANAKA (Eds.), CERN-2017-002 (2016).
- [34] A. BAZAVOV *et al.*, *Phys. Rev. D*, **98** (2018) 054517.
- [35] ATLAS COLLABORATION, ATL-PHYS-PUB-2021-039 (2021), <https://cds.cern.ch/record/2788490>.